Optimal deployment of resources for maximizing impact in spreading processes

Andrey Y. Lokhov[a,1] **and David Saad**[b]

[a]Center for Nonlinear Studies and Theoretical Division T-4, Los Alamos National Laboratory, Los Alamos, NM 87545; and [b]The Nonlinearity and Complexity Research Group, Aston University, Birmingham B4 7ET, United Kingdom

Edited by Giorgio Parisi, University of Rome, Rome, Italy, and approved July 24, 2017 (received for review September 1, 2016)

The effective use of limited resources for controlling spreading processes on networks is of prime significance in diverse contexts, ranging from the identification of "influential spreaders" for maximizing information dissemination and targeted interventions in regulatory networks, to the development of mitigation policies for infectious diseases and financial contagion in economic systems. Solutions for these optimization tasks that are based purely on topological arguments are not fully satisfactory; in realistic settings, the problem is often characterized by heterogeneous interactions and requires interventions in a dynamic fashion over a finite time window via a restricted set of controllable nodes. The optimal distribution of available resources hence results from an interplay between network topology and spreading dynamics. We show how these problems can be addressed as particular instances of a universal analytical framework based on a scalable dynamic message-passing approach and demonstrate the efficacy of the method on a variety of real-world examples.

optimal control of spreading processes | dynamic resource allocation | message-passing algorithms | influence maximization | mitigation of epidemic outbreak

Spreading corresponds to omnipresent processes describing a vast number of phenomena in social, natural, and technological networks (1–4) whereby information, viruses, and failures propagate through their edges via the interactions between individual constituents. Spreading cascades have a huge impact on the modern world, be it negative or positive. An 11-min power grid disturbance in Arizona and California in 2011 led to cascading outages and left 2.7 million customers without power (5). As many as 579,000 people around the world could have been killed by the H1N1 influenza pandemic, characterized by a rapid spreading through the global transportation networks (6). The US economy losses from the 2008 financial crisis resulting from cascading bankruptcies of major financial institutions are estimated at $22 trillion (7). Therefore, it is not surprising that efficient prediction and control of these undesired spreading processes are regarded as fundamental questions of paramount importance in developing policies for optimal placement of cascade-preventing devices in power grid, real-time distribution of vaccines and antidotes to mitigate epidemic spread, regulatory measures in interbanking lending networks, and other modern world problems, such as protection of critical infrastructures against cyberattacks and computer viruses (8).

On the other hand, spreading processes can also be considered beneficial. The Ice Bucket Challenge campaign in social networks raised $115 million donations to the ALS Association fighting amyotrophic lateral sclerosis, in particular due to a significant involvement of celebrities acting as "influencers" (9). In the context of political campaigning, there are already winners (10, 11) and losers, and this division is likely to become more pronounced and critical in the future (12). Winners are those who use communication and social networks effectively to set the opinions of voters or consumers, maximizing the impact of scarce resources such as activists or advertisements by applying control to the most influential groups of nodes at the right time, while losers will spend their resources suboptimally, relying on intuition and serendipity. Additional examples of domains where optimal resource allocation plays a crucial role in enhancing the effect of spreading include viral marketing campaigns (13); targeted chemically induced control of dynamic biological processes (14); drug discovery (15); and even gaining military advantage through the propagation of disinformation (16). All of these applications share several important common properties such as restricted budget, finite time windows for dynamical control interventions, and the need for fast and scalable optimization algorithms which can be deployed in real time.

There exists a large body of work on optimal resource deployment in various spreading settings. A widely addressed formulation focuses on identifying influential spreaders (i.e., nodes that play an important role in the dynamical process). Identification is often done by using different centrality measures related to the topology of the underlying interaction network, including selection strategies based on high-degree nodes (17), neighbors of randomly selected vertices (18), betweenness centrality (19), random-walk (20), graph-partitioning (21), and k-shell decomposition (22), to name a few. It is quite natural that algorithms based exclusively on topological characteristics appear to have variable performance depending on particular network instances and dynamical models used (23, 24). Another line of work consists in studying the nondeterministic polynomial time (NP)-complete problem of network dismantling (25–27): The underlying reasoning is that removal of key nodes fragments the giant component and hence is likely to prevent a global percolation of the contagion. The localization of an optimal immunization set has been addressed by using a belief

Significance

Spreading processes play an increasingly important role in marketing, opinion setting, and epidemic modeling. Most existing algorithms for optimal resource allocation in spreading processes are based on topological characteristics of the underlying network and aim to maximize impact at infinite time. Clearly, realistic and efficient real-time allocation policies should consider both network properties and details of the dynamics; additionally, control may be applied only to a restricted set of accessible nodes, and impact should be maximized in a limited time window. We introduce a probabilistic targeting framework that incorporates the dynamics and encompasses previously considered optimization formulations. It is based on a scalable dynamic message-passing approach that allows for the solution of large real-world network instances.

Author contributions: A.Y.L. and D.S. designed research, performed research, contributed new reagents/analytic tools, analyzed data, and wrote the paper.

The authors declare no conflict of interest.

This article is a PNAS Direct Submission.

[1]To whom correspondence should be addressed. Email: lokhov@lanl.gov.

This article contains supporting information online at www.pnas.org/lookup/suppl/doi:10.1073/pnas.1614694114/-/DCSupplemental.

propagation algorithm built on top of percolation-like equations for SIR (susceptible, infected, recovered) and SIS (susceptible, infected, susceptible) models (28), based on cavity method techniques developed previously for deterministic threshold models (29, 30). This formulation is close to the problem of finding optimal seeds [i.e., the smallest set of initial nodes which maximizes the spread asymptotically (13)]. It was rigorously analyzed (31, 32) for two simple diffusion models with a special submodularity property, independent cascade (IC) and linear threshold, and was shown to be NP-hard for both. A greedy algorithm based on a sampling subroutine has been explored for the IC model (33) in the setting of a finite time horizon. For other spreading models, the impact maximization problem at finite time and resources has been addressed in the setting of optimal control as reported in a recent survey (34). However, only deterministic mean-field dynamics have been considered so far; this approximation ignores the topology of the specific network considered and yields nondistributed solutions to the control problem.

All of these techniques consider the problem of static (open-loop) resource allocation, preplanned at some initial time. A less explored direction consists of developing an online policy of assigning a limited remedial budget dynamically based on real-time feedback, also known as a closed-loop control. The impact of vaccination of the largest degree nodes or of those with the largest number of infected neighbors was investigated in refs. 35 and 36, while an alternative strategy is focused on the largest reduction in infectious edges (37). Finally, an online policy based on solution of the minimal maxcut problem was introduced (38), where optimization is carried out with respect to the expected time to extinction of the SIS epidemic.

We introduce a general optimization formulation which accommodates both dynamical and topological aspects of the problem and which allows for a broad range of objectives. The framework facilitates the optimization of objective functions beyond the maximization or minimization of the spread, including: targeting specific nodes at specific times given a subset of accessible nodes; a limited global budget, possibly distributed over time; and an optimal dynamic vaccination strategy using feedback from the spreading process. The problem is stated in a dynamical control setting with finite-time horizon that requires an explicit solution of the dynamics, which is addressed via a distributed message-passing algorithm. We test the efficacy of the method on particular synthetic optimization problems as well as on a set of real-world instances.

Model

A large number of spreading models have been suggested in the literature to describe stochastic dynamical processes in epidemiology, information and rumor propagation, and cascades in biological and infrastructure networks (2–4). They all share the same common features: The nodes transition from inactive to active state due to spontaneous activation mechanism associated with the nodes themselves or due to interactions with active neighbors through the network edges. As an illustration of our approach, we have chosen a popular stochastic spreading process known as the SIR model, which is often used to describe propagation of infectious diseases or information spreading (2). More precisely, we consider a modified version of the discrete-time SIR model defined as follows. A node i in the interaction graph $G = (V, E)$, where V denotes the set of nodes and E is the set of pairwise edges, can be found at time step t in either of three states σ_i^t: "susceptible" $\sigma_i^t = S$, "infected" $\sigma_i^t = I$ or "recovered" $\sigma_i^t = R$. At each time step, an infected (or, depending on the application domain, informed or active) individual i can transmit the activation signal to one of its susceptible (respectively, uninformed or inactive) neighbors j with probability α_{ij}, associated with the edge connecting them. Independently of the interaction between nodes, a node i in state S at time t can turn active, assuming state I with probability $\nu_i(t)$, or spontaneously become recovered (uninterested, protected) with probability $\mu_i(t)$. The first mechanism corresponds to a node activation due to an external influence such as advertisement in the context of information spreading. In the case of the epidemic spreading, the second mechanism models the effect of vaccination: Once a node goes to the protected R state, it becomes immune to the infection at all times. These probabilistic transmission rules at each time step t can be summarized using the following schematic rules (depicted in Fig. S1):

$$S(i) + I(j) \xrightarrow{\alpha_{ji}} I(i) + I(j), \qquad [1]$$

$$S(i) \xrightarrow{\nu_i(t)} I(i), \qquad S(i) \xrightarrow{\mu_i(t)} R(i). \qquad [2]$$

In the definition of the dynamic rules **[1]** and **[2]**, $\nu_i(t)$ and $\mu_i(t)$ represent control parameters we could manipulate with a certain degree of freedom defined by a particular instance of the problem. Notice that these control parameters act in opposite directions, expediting or hindering the propagation process. In all examples considered, we typically study either the susceptible, infected (SI) model with the ν-mechanism as a paradigm for the propagation of information, or the modified SIR dynamics with the vaccination μ-mechanism as a model of the epidemic spreading. In what follows, we assume that the spreading couplings α_{ij} are known (or can be estimated) and are fixed in time. In some applications, α_{ij} may vary in time (e.g., this is true for temporal networks) or may represent a set of control parameters themselves. We outline such scenarios in *Discussion*; the optimization scheme presented below can be straightforwardly generalized to include time-varying and edge-related control parameters. However, for simplicity, we will only present optimization involving node-related control parameters.

To quantify the success of the spreading process, one may look for instance at the expected spread (the total number of infected nodes) at final time horizon T, $\mathcal{S}(T)$, given by

$$\mathcal{S}(T) = \mathbb{E}\left[\sum_{i \in V} \mathbb{1}[\sigma_i^T = I]\right] = \sum_{i \in V} P_I^i(T), \qquad [3]$$

where the expectation is taken with respect to the realization of the stochastic dynamics and $P_I^i(T)$ denotes the marginal probability of node i to be found in state I at time T. The quantities $P_S^i(T)$ and $P_R^i(T)$ can be defined in a similar way for the susceptible and recovered states, respectively. Hence, it is important to understand how to compute approximately the marginal probabilities $P_\sigma^i(t)$ on a given network, with σ representing the corresponding state; note that in the general case, an exact evaluation of marginals in the SIR model is an NP-hard problem (39). We use the recently introduced dynamic message-passing (DMP) equations (40–42), which provide estimates of the probabilities $P_\sigma^i(t)$ with a linear computational complexity in the number of edges and time steps. These equations are derived under the assumption of a locally tree-like network and provide asymptotically exact estimates on sparse random graphs. When applied to real-world loopy networks, the DMP algorithm typically yields an accurate prediction of marginal probabilities as validated empirically (42) for a large class of spreading models on real-world networks. In *Methods*, we provide an intuitive derivation of the corresponding DMP equations for the considered modified SIR model. An example of the DMP performance on real-world networks is provided in Fig. 1, where the method predictions are compared with values obtained through extensive Monte Carlo simulations of the SIR dynamics on a network of flights between major US hubs (a detailed description of this dataset is provided below and in *SI Text*). The accuracy of marginals estimation supports the use of the DMP equations at the core of our optimization algorithm.

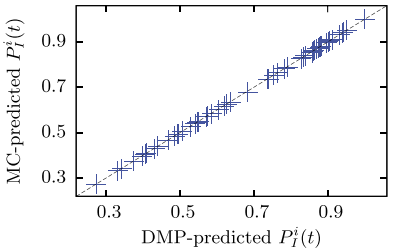

Fig. 1. Performance of DMP equations for the modified SIR model on a network of flights between major US airports. The network represents $M = 383$ flight routes between the $N = 61$ largest US hubs. The weights α_{ij} are proportional to the average number of transported passengers on each route and are distributed in the interval [0.05, 0.5]; ν_i and μ_i are generated at random in the range [0, 0.1]. The scatter plot represents marginal probabilities $P_I^i(T)$ obtained from the DMP equations and by averaging over 10^7 Monte Carlo (MC) simulations. There is one randomly selected active node at the initial time, and the dynamics is simulated for $t = 5$ time steps.

Optimization Framework

We formulate the dynamic allocation of resource as a general optimization problem with respect to an objective function $\mathcal{O}$ and a set of constraints associated with the budget of available resources $\mathcal{B}$, accessible values of control parameters $\mathcal{P}$, initial conditions $\mathcal{I}$, and the dynamical model equations $\mathcal{D}$. We use the Lagrangian formulation of the constrained optimization problem:

$$\mathcal{L} = \underbrace{\mathcal{O}}_{\text{objective}} + \underbrace{\mathcal{B} + \mathcal{P} + \mathcal{I} + \mathcal{D}}_{\text{constraints}}. \quad [4]$$

Let us discuss the form of each of the terms in the expression [**4**].

$\mathcal{O}$: Many objective functions of interest relate to the delivered information *at particular times* defined for each node. So, for the general case we define:

$$\mathcal{O} = \mathbb{E}\left[\sum_{i \in U} \mathbb{1}[\sigma_i^{t_i} = I]\right] = \sum_{i \in U} P_I^i(t_i), \quad [5]$$

where t_i is the required activation time for node i and the sum is over the subset of nodes $U \subset V$ that is required to be activated. We refer to this general formulation as the targeting problem. The popular problem of maximizing the total spread $\mathcal{S}(T)$ is a special case whereby $U = V$ and $t_i = T$ for all $i \in V$.

$\mathcal{B}$: In many relevant situations, resources are not fully available at a given time, but rather become available on the fly, and their amount may vary across the time steps. For example, it takes some time to develop and produce the vaccines, or the advertisement budget can be allocated in stages depending on the success of the campaign. Hence, we define the budget constraints in the following form:

$$\sum_{i \in V} \nu_i(t) = B_\nu(t), \quad \sum_{i \in V} \mu_i(t) = B_\mu(t), \quad [6]$$

where $B_\nu(t)$ and $B_\mu(t)$ denote the available total budget for the control parameters $\nu_i(t)$ (spontaneous infection) and $\mu_i(t)$ (recovery through vaccination) at time t. The constraint $\mathcal{B}$ reads

$$\mathcal{B} = \sum_{t=0}^{T-1} \lambda_B^\nu(t) \left[\sum_{i \in V} \nu_i(t) - B_\nu(t)\right], \quad [7]$$

with a similar expression for the parameters $\mu_i(t)$, where $\lambda_B^\nu(t)$ and $\lambda_B^\mu(t)$ are the associated Lagrange multipliers, respectively. Allocation of budget only at the initial time corresponds to the optimal seeding problem.

$\mathcal{P}$: In an unrestricted scenario, where all nodes are accessible, control parameters associated with node i, $\nu_i(t)$ and $\mu_i(t)$ may take arbitrary values from zero to one depending on total budget. However, in realistic situations access level to different nodes may differ: For example, only a subset $W \subseteq V$ of nodes may be controllable together with additional restrictions on parameter values. The parameter block $\mathcal{P}$ is introduced to enforce parameters $\nu_i(t)$ to take values in the range $[\underline{\nu_i^t}, \overline{\nu_i^t}]$ at each time step. This can be accomplished with the help of barrier functions, widely used in constrained optimization, assuming the form

$$\mathcal{P} = \epsilon \sum_{t=0}^{T-1} \sum_{i \in V} \left(\log\left[\nu_i(t) - \underline{\nu_i^t}\right] + \log\left[\overline{\nu_i^t} - \nu_i(t)\right]\right), \quad [8]$$

where ϵ is a small regularization parameter chosen to minimize the impact on the objective $\mathcal{O}$ in the regime of allowed $\nu_i(t)$ values, away from the borders. An equivalent expression can be written for the constraints on the $\mu_i(t)$ values.

$\mathcal{I}$ and $\mathcal{D}$: Finally, the constraints $\mathcal{I}$ and $\mathcal{D}$ enforce the given initial conditions and dynamics of the system via the associated Lagrange multipliers. For example, if no active individuals are present at the initial time, then we set $P_I^i(0) = 0$ for all nodes using the constraint set $\mathcal{I}$; if some infected or recovered nodes are present, they assume an initial value 1 for the respective marginal probabilities. The set $\mathcal{D}$ encodes the evolution of the marginal probabilities with the DMP equations, as explained in *Methods*.

The extremization of the Lagrangian [**4**] is done as follows. Variation of $\mathcal{L}$ with respect to the dual variables (Lagrange multipliers) results in the DMP equations starting from the given initial conditions, while derivation with respect to the primal variables (control and dynamic parameters) results in a second set of equations, coupling the Lagrange multipliers and the primal variable values at different times. We solve the coupled systems of equations by forward–backward propagation, a widely used method in control, as well as for learning and optimization in artificial neural networks (43), detailed in *Methods* and schematically illustrated in Fig. 2. This method has a number of advantages compared with other localized optimization procedures such as gradient descent and its variants. In particular, it is simple to implement, is of modest computational complexity due to the gradient-free nature of the optimization, does not require any adjustable parameters, and is less prone to being trapped in local minima since the optimization is performed globally (44).

In what follows, we illustrate this general optimization framework on three practical case studies: driving dynamic trajectory of a spreading process in time through a set of targets (targeting problem), selecting an optimal set of initial seeds for a maximum dissemination of influence or information (influence maximization problem), and online closed-loop distribution of vaccines for stabilizing the spread of an infection (online mitigation of epidemic spreading). In each of these examples, we show how our algorithm can be used to solve particular problems from social or biological sciences, compare the performance to existing techniques (where competing algorithms exist), and indicate a number of other prospective applications.

Case Study: Guiding Spreading Through Desired Targets

Targeting is quite a general task and can provide a useful problem formulation in many application domains where the underlying dynamics is governed by a set of nonlinear differential or difference equations. The nature of these applications can be very diverse: They range from targeting biochemical cascades to treat cancer (45, 46) and controlling the trajectories of brain dynamics among states characterized by the activation of various cognitive systems (47) to maximizing the species abundance by targeted interventions in food webs (48) and ecological mutualistic networks (49). In the context of spreading processes, targeting tasks appear in several problems of social importance: online

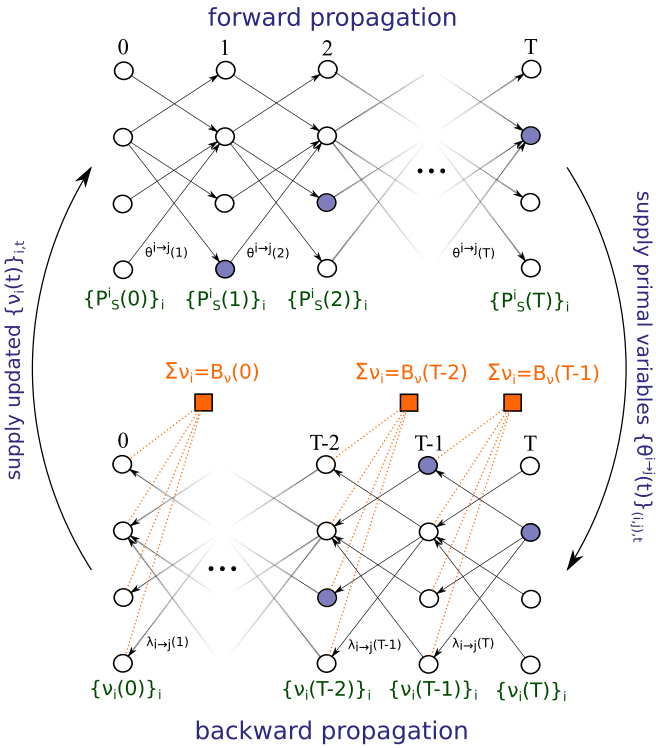

Fig. 2. Schematic representation of the forward–backward propagation algorithm. The optimization scheme is presented in the case of the SI model with spontaneous activations due to the ν-mechanism. The state of the network is presented at each time step; nodes to be targeted at particular time steps are colored in blue. Given the current values of the control parameters $\{\nu_i(t)\}_{i\in V}$, the marginal probabilities $\{P^i(t)\}_{i\in V}$ are computed in the forward propagation stage through the exchange of messages $\{\theta^{i\to j}(t)\}_{(ij)\in E}$ along the edges of the graph between neighboring nodes, according to the update rules of the DMP equations. In the backward propagation phase, the nodes exchange the dual messages, represented by the Lagrange multipliers $\{\lambda_{i\to j}(t)\}_{(ij)\in E}$ associated with the primal variables. At each time step, the parameters $\{\nu_i(t)\}_{i\in V}$ are updated according to the backward dynamic equations, subject to the budget constraints, depicted by orange squares, and the targeting requirements. The two stages are iterated until convergence of the algorithm to a fixed point, or for a predefined number of steps.

optimal distribution of the mitigation budget prioritizing the "too big to fail" financial institutions due to the financial contagion (50) modeled as a spreading process (51, 52); strategy for the active cyber defense dynamics (53) based on spreading "benign" worms (54) for targeting the infected computers and servers; and development of the optimal policy (55) for the acceleration of the diffusion of innovations (3). Let us also mention that targeting can provide algorithms to solve a number of related problems. For instance, identifying the origin of the spreading process from measurements at sparsely located sensors at different times (56) is a difficult problem that has been addressed by other approaches (57, 58), but can be equally viewed as optimally allocating a budget at time 0 to target the sensor nodes at specific times that correspond to the times when measurements were taken.

Despite a wide applicability of the targeting task, until now, no general algorithm is known to drive efficiently the activation process through desired states. In this section, we illustrate the performance of the DMP approach using the general targeting formulation, one of the features of the suggested framework. As a toy example, we consider disinformation spreading on a small network extracted from the 9/11 case study of terrorist associations, representing the established trusted contacts between the hijackers (59). A number of studies suggested methods for destabilizing covert networks; see refs. 60 and 61 for a literature survey. Our rationale in using this example is the ability to demonstrate the targeted activation of nodes at given times, which corresponds to the intentional exposure of the respective individual to misinformation, and considered as one of the protective measures undertaken by the counterterrorism intelligence (62). The spontaneous activation parameters have the interpretation of an aggregated influence [e.g., through counternarratives diffused through the social media by external operatives and special agencies such as the Center for Strategic Counterterrorism Communications (63)]; the resources for such interventions are limited by a certain budget per time step. In the original study (59), the networks of terrorist contacts have been analyzed from the leadership identification perspective: A removal of just several nodes is sufficient to break the network. In our example, the targets specified at each time step may reflect the order of priority in which the nodes should be influenced, in particular those having unique skills for the planned operation (e.g., pilots in the 9/11 example); similar argument has been put forward in the study of the criminal networks (64).

More specifically, we assume that the spreading dynamics follows a particular case of the dynamical model with $\mu_i(t) = 0\,\forall\, t$ and $i \in V$, corresponding to the SI model with controlled spontaneous transition to the informed state I due to external influence via the control parameters $\nu_i(t)$. The activation of nodes is required in a predefined priority order, targeting selected nodes at specific times. The DMP-based optimization scheme converges to a unique optimal solution within a few forward–backward iterations. The resources are allocated dynamically over time such that the activation path meets the targeting requirements, as reported in Fig. 3: $P_I^i(t_i) > 0.95$ is achieved at all nodes, with the majority of nodes targeted with probability one. Our algorithm is computationally efficient and can be applied to very large network instances, as we show below.

Case Study: Influence Maximization via Seed Selection

The seeding problem, which deals with the optimization over the initial condition only, can be viewed as a particular instance of the targeting formulation. A classical formulation of the seeding task consists of finding the best K nodes which, when activated at initial time, would lead to the maximum spread at time T (31). With the DMP approach being inherently probabilistic,

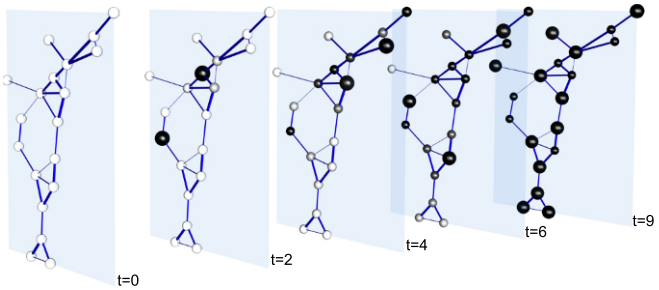

Fig. 3. Optimal targeting with the DMP algorithm on a small network of terrorist associations. Edge thickness indicates the strength of the corresponding pairwise transmission probability α_{ij}, generated uniformly at random in the interval [0, 1]. The size of nodes relates to the time activation requirements: Large nodes should be activated by the corresponding time. In this example, two chosen nodes should be activated at time $t = 2$, another two nodes by time $t = 4$, three particular nodes by time $t = 6$, and all remaining nodes by time $t = 9$; available budget for each time step has been fixed to $B_\nu(t) = 0.1\,N$. Color intensity (gradually from white to black) indicates the value of the marginal probabilities $P_I^i(t)$ which result from the dynamics using the optimal distribution of resources provided by the DMP algorithm. The visualization has been created by using the MuxViz software (65).

we consider a slightly more general (and arguably more realistic in applications) space of initial conditions. Assume that the initial condition is generated probabilistically, so that each node i at the initial time is infected independently with probability p_i; the conventional formulation is recovered when p_i take only binary values, zero or one, and $\sum_{i\in V} p_i = K$. In the considered formulation involving control parameters $\nu_i(t)$, we optimize over the set of arbitrary probabilities $p_i \in [0, 1]$: Setting the initial conditions for such p_i at time $t = 1$ is equivalent to fixing the values of the parameters $\nu_i(0)$ at the auxiliary time $t = 0$ in the system where all nodes are in state S. Therefore, an optimal distribution of the budget $B_\nu(0)$ (not necessarily integer) at time $t = 0$ would thus lead through spontaneous infection to the maximum spread $\mathcal{S}(T + 1)$. In *SI Text*, we present an example of the influence maximization problem in a network of relations between political parties illustrated in Fig. S2. As in the previous example for the targeting problem, the forward–backward optimization scheme quickly converges to a unique ground-truth optimal solution, which in this small test case can be established by a direct maximization of the explicit symbolic form of the objective function $\mathcal{O}$; see Fig. S3 for additional details. This small-scale example hence serves as a validation of our optimization procedure.

A large number of topology-based algorithms have been designed to address the seeding problem, mostly in the case of the homogeneous transmission probabilities (17–22, 25, 28). To test the efficacy of the DMP-optimization approach on large-scale instances, we compare its performance to that of popular heuristics for the restricted setting of near-deterministic spreading. The choice for this setting is motivated by the fact that one can devise a simple algorithm providing a good approximation to the ground-truth solution, which can serve as a benchmark for comparing different algorithms, and a number of centrality techniques (17, 22, 25) selecting combinations of high-degree nodes should perform well in this case; see *SI Text* for a detailed discussion of methods used for comparison, implementations, and additional remarks. The results of comparisons on a number of real-world and synthetic networks of different sizes and topologies are summarized in Table 1 and Fig. 4. In *SI Text*, we also discuss additional numerical results for the case of heterogeneous couplings, assessing the performance of the DMP method compared with a natural generalization of centrality algorithms to the heterogeneous setting. The main message emerging from these tests can be formulated as follows: Although the DMP method has not been optimized for the seeding problem and does not rely explicitly on topological features such as targeting high-degree nodes, we find that it is close to the best-performing heuristics in all cases, showing a consistently good performance. This suggests that the DMP algorithm performs well also for more general dynamic resource allocation problems for which other principled methods do not exist, such as targeting problems described in the previous section and global-time closed-loop control policies discussed further.

An interesting observation is that in the case of large network instances, the forward–backward iteration scheme no longer converges to a unique optimum as in the case of small networks considered previously. Instead, the algorithm makes large "jumps" on the manifold representing different control-parameter distributions that obey the budget constraints [**6**]: This is a manifestation of the NP-hardness of the problem with a more complex optimization landscape and a multitude of local optima. The presence of many solutions with comparable costs is an indication that it is arguably more appropriate to view the different seeding sets as a collective phenomenon, rather than assigning "influence" measure to individual nodes. In terms of computational complexity, solving the dynamics with DMP is linear in T and $|E|$; the number of forward–backward iterations is typically small and can be controlled, as explained in *Methods*. Let us also point out that the DMP-estimated marginals provide a natural and convenient measure for comparing the performance of different algorithms in the finite time horizon setting, especially on large graphs with millions of nodes where running extensive Monte Carlo simulations is computationally prohibitive.

Case Study: Online Mitigation of Epidemic Spreading

To illustrate the suitability of the DMP algorithm to online deployment of resources in a dynamic setting with feedback, we use a prototypical example: developing an effective mitigation policy for confining an infectious disease—a practical and challenging question of public concern. A modified SIR model with vaccination is an appropriate dynamic model in this case, where the $\nu_i(t)$ variables are set to zero, and the parameters $\mu_i(t)$ play the role of vaccination control, allowing the susceptible nodes to assume a protected state R. The vaccination mechanism modeled via an S to R transition has been studied in the context of the SIR-type spreading models in refs. 70 and 71. Note that extension to other spreading models with different vaccination mechanisms is straightforward, as pointed out in *Discussion*. In contrast to the targeting and seeding problems, the initial conditions (origin of the epidemic) are specified in this setting, and the vaccination budget has to be allocated dynamically according to the current state of the spreading process (monitored at each time step) to suppress the epidemic. The goal is to deploy

Table 1. Comparison of the DMP algorithm for the seeding problem in the setting of near-deterministic dynamics with popular heuristics on various real-world and artificial networks

Network	N	M	Random	HDA	k-shell	CI_2	CI_4	Uniform	DMP	Covering
Road EU	1174	1417	0.305	0.480	0.163	0.500	0.468	0.324	0.513	0.565
Protein	2361	6646	0.736	0.863	0.772	0.861	0.838	0.752	0.856	0.903
US power grid	4941	6594	0.367	0.602	0.206	0.605	0.565	0.397	0.601	0.684
GR collaborations	5242	14,484	0.565	0.644	0.291	0.660	0.658	0.634	0.710	0.796
Internet	22,963	48,436	0.880	0.998	0.987	0.996	0.994	0.891	0.972	0.995
Web-sk	121,422	334,419	0.645	0.833	0.242	0.751	0.734	0.699	0.837	0.937
Scale-free	500,000	397,848	0.214	0.398	0.220	0.372	0.323	0.215	0.321	0.427
Erdős-Rényi	500,000	750,000	0.447	0.681	0.494	0.677	0.679	0.446	0.704	0.719

First three columns on the left of the table provide topological information on the networks considered (66–69). In the remaining columns on the right are presented values of the normalized total spread $\mathcal{S}(T)/N$ at time $T = 3$, given homogeneous transmission probabilities $\alpha_{ij} = \alpha = 0.99$ and the total available budget $B_\nu(0) = 0.05\,N$, for the different algorithms: assignment to randomly-selected nodes, an adaptive version of the high-degree strategy of ref. 17 (HDA) and of the k-shell decomposition (22), collective influence $(\mathrm{CI})_l$ (25) (with $l = 2$ and $l = 4$), uniform assignment, the DMP algorithm, and the Covering algorithm which has a near-optimal performance in this case and serves as a benchmark. Description of these algorithms along with the implementation details is provided in *SI Text*. For different test cases, solutions obtained by DMP span the range between delocalized and node-centric assignments and are on par with the best-performing centrality heuristics. The results presented in this table are graphically summarized in Fig. 4. See *SI Text* and Table S1 for analogous comparisons in the case of heterogeneous couplings.

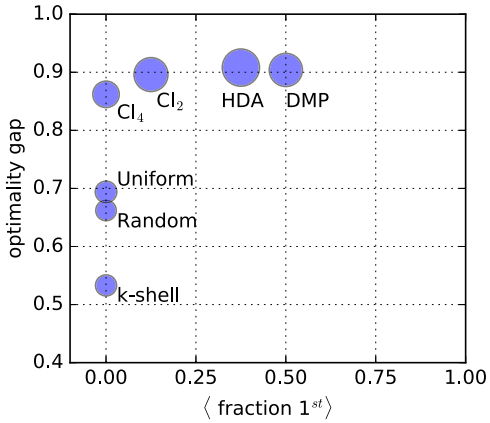

Fig. 4. Comparison of different algorithms for the seeding problem. This figure summarizes in a graphical form the results of comparisons between several seeding algorithms for the near-deterministic spreading on a number of real and synthetic network instances; details and raw numbers are provided in Table 1. Each algorithm is represented by a circle, centered at the point with coordinates (x, y), with x being the fraction of test cases for which the algorithm had the best performance, and y defined as the average "optimality gap" [i.e., average result normalized by the value output by the specially designed Covering strategy (near-optimal in this setting, as explained in *SI Text* and in Fig. S4) for each of the networks studied]. The ideal algorithm for this problem should lie in the right upper corner with coordinates (1, 1). The size of each circle is inversely proportional to the average rank of the corresponding algorithm. The high degree adaptive (HDA) policy shows a slightly lower optimality gap compared with DMP; nevertheless, overall, the DMP approach (which is not specifically optimized for the seeding problem) demonstrates a consistently good performance; this is a premise for its proper performance in general large-scale general dynamic resource allocation problems.

the resources optimally so that the total number of infected nodes $\mathcal{S}(T)$ at the final time is minimized. The assumption of a time-distributed budget $B_\mu(t)$ is highly reasonable due to the restricted vaccine availability.

Previously developed real-time strategies for mitigating contagion on a given network (35, 37, 38) explored policies that were based on topological characteristics of the graph under the assumption of homogeneous transmission probabilities. The common denominator of existing approaches consists in local interventions, which ensure the islanding of infected nodes. We generalize the methods (35, 38) to the case of heterogeneous transmission probabilities using a "high-risk" (36) ranking of susceptible nodes at time t according to their probability of getting infected at the next time step. This measure is defined in our case as

$$P_i^t(S \to I) = 1 - \prod_{j \in \partial i} (1 - \alpha_{ji} \mathbb{1}[\sigma_j^t = I]), \qquad [9]$$

where ∂i denotes the set of neighbors of a susceptible node i. A reasonable local intervention strategy for benchmarking consists of distributing the vaccination budget to priority nodes with a high-risk measure [**9**]. This algorithm will be referred to as the greedy strategy.

Several policies can be conceived by using the DMP optimization framework. As a reference, we consider the planned deployment of resources which does not take into account feedback from an actual realization of the process, but merely follows the solution of the dynamic resource allocation problem with a specified initial condition. Two other closed-loop strategies take into account the real-time information on the spreading process, using the seeding formulation as a subroutine: (*i*) The first, termed "DMP-greedy," is close in spirit (but differs in the algorithmic implementation, based here on the DMP optimization framework) to the greedy algorithm and uses the current state of the epidemic as the initial condition, aiming to minimize the spread at the next time step only. (*ii*) The second uses the full power of the DMP framework by exploiting the up-to-date information available to reinitialize the dynamics at each time step t for allocating the resources at the next time step $t + 1$, by running the optimization procedure for the remaining $T - t$ time steps. This "DMP-optimal" policy is similar to the planned strategy, but takes advantage of the new information available from the realization of the process.

We compare these strategies for the case of infection spreading mediated by air traffic, which has been recognized as an important factor facilitating the spread of infectious diseases (72) and thus plays a major role in recent world's pandemics (73). As a particular example, we study the real-world transportation network of busiest flight routes between major US airports, extracted from the Bureau of Transportation Statistics (BTS) data (74) and depicted in Fig. 5*A*. The use of the modified SIR model in this case is justified by the fact that this type of spreading models has been widely used for modeling a traffic-mediated epidemic (75, 76). We use a plausible assumption that the infection transmission probability associated with a link between airports is proportional to the number of passengers carried along this route (see *SI Text* for a detailed description of the network and data used). The "vaccination" interventions on this network can be interpreted as quarantine measures taken in different airports using the updates on the newly infected cases. Indeed, containment measures and travel restrictions have been pointed out as important factors limiting the spread of an epidemic (77). In the simulations, we assume that the epidemic starts at the largest airport hub of Atlanta.

The comparison of different mitigation algorithms is given in Fig. 5*B*, showing the average number of infected sites as a function of time under different mitigation strategies. As expected, the DMP-optimal scheme represents the best performing policy, which leads to stabilization of the expected number of infected nodes by $t = 6$, at a lower level compared with the greedy algorithm that optimizes the spread at the next time step only. Notice that on a short time scale, the greedy algorithm has a slightly better performance, which represents a typical situation when localized and immediate optimal decisions lead ultimately to suboptimal global optimization results; an illustration is provided in Fig. 5*C*.

Discussion

We introduce an efficient and versatile optimization framework for solving dynamic resource allocation problems for spreading processes, which allows for the synthesis of previously studied settings within a general targeting formulation. This probabilistic framework allows one to study problems that involve a finite-time horizon, which requires an explicit solution of the dynamics, the targeting of specific nodes at given times in both open- and closed-loop setting, as well as scenarios where only a subset of the nodes is accessible. This is done in our scheme by using the DMP equations for spreading processes. Although in this work we focus on examples involving the discrete-time modified SIR model, the approach can be straightforwardly applied to the case of continuous dynamics (the continuous formulation is expounded in *SI Text*) and to other cascading models, including but not limited to threshold models (29, 41) and rumor dynamics (42). Another possible application area of the present framework relates to systems defined on temporal graphs, where network dynamics can be encoded into the time-dependent coefficients $\alpha_{ij}(t)$ within the existing framework.

Although we show that the method can be used in the case where transmission probabilities are uniform and only the detailed topology of the network is known, its major advantage consists of the ability to incorporate efficiently detailed

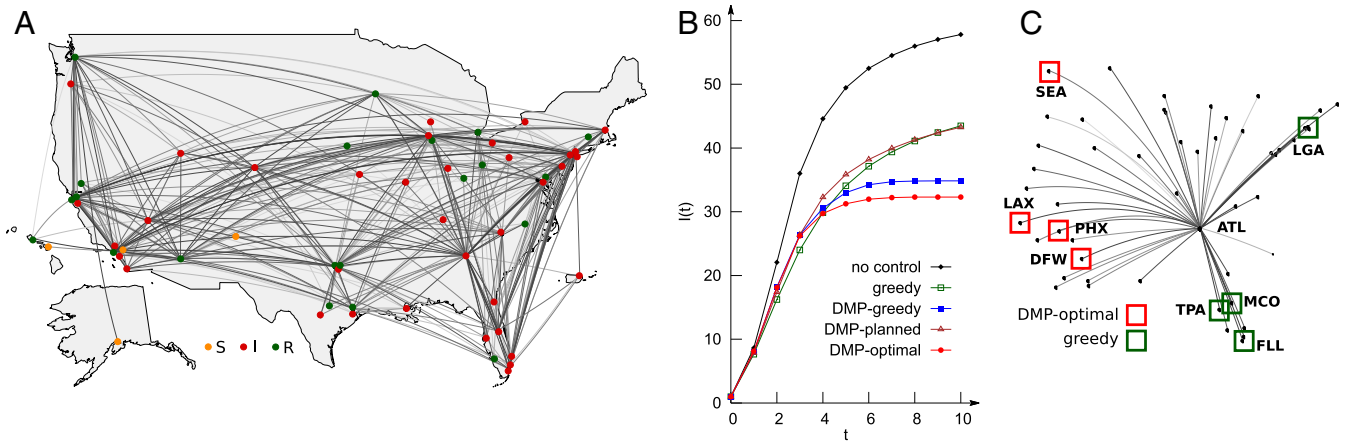

Fig. 5. Online mitigation of air-traffic mediated epidemic on the network of flights between major US hubs. (*A*) A geographical layout of the air transportation subnetwork extracted from the BTS data (74). The transmission probabilities are indicated by the thickness of the corresponding edges, which are proportional to the aggregated traffic between airports. Different colors of airports (yellow, red, and green) represent an outcome of a single realization of the spreading dynamics (nodes in the susceptible, infected, and recovered states, respectively) under the DMP-optimal policy. (*B*) Comparisons of mitigation strategies show the average number of infected sites as a function of time, averaged over 100 random realizations of the dynamics, for the different policies. In the simulations, the epidemic starts at the largest airport hub of Atlanta; a budget of $B_\mu(t) = 0.05\ N$ is available at each time step, and the objective is to suppress the epidemic by $T = 10$. The DMP-optimal algorithm demonstrates the best performance in the number of infected nodes at time T. (*C*) An illustration of a radically different decisions taken by the DMP-optimal and greedy algorithms already at the first step of the optimization: The greedy policy chooses to vaccinate nodes which are most "in danger" at the next time step, while the decision done by the DMP-optimal scheme takes into account the forecasted evolution of the dynamics.

information on transmission probabilities when such prior information is available, or can be either estimated (as in the examples of flight transportation networks, given above, and Slovene political parties, treated in *SI Text*) or learned from past observations of the dynamics (78, 79). Despite the global budget constraints involving all network nodes, the resulting message-passing scheme is fast and distributed, requiring a number of operations which grows linearly in time and with respect to the number of edges in the network. An attractive property of the suggested framework is its versatility: Instead of optimizing the spread given a fixed budget, one can minimize the budget needed to meet certain requirements on the spread, imposed as a constraint in the Lagrangian formulation. Another interesting scenario is the optimization over the spreading parameters α_{ij}: This formulation is useful in the design of technological networks or for mitigation of an epidemic by removing and adding links in the graph. It would be interesting to apply the presented optimization scheme to the percolation-type equations describing the asymptotic $T \to \infty$ limit of the spreading dynamics with heterogeneous couplings.

The optimization method used is based on changes to the entire trajectory, instead of taking incremental improvement steps in the direction of the gradient; thus, the suggested algorithm results in large steps and arguably explores more effectively the parameter space. The fact the optimization is gradient-free represents an additional advantage from the point of view of the computational complexity in problems where the gradient is hard to compute; for instance, in the case of the DMP equations presented in this work, computation of the gradient requires $O(|E|NT)$ operations for the node-related control parameters, and $O(|E|^2 T)$ operations for the edge-related parameters, which would make the algorithm impractical for large networks. This property of the optimization scheme makes it an attractive option for the DMP-based learning algorithms (78), where the gradient computation represents a scalability bottleneck. The solution of the learning problem in the presence of hidden nodes together with the introduced targeting formulation would make it possible to construct the DMP-based artificial learning architectures.

Notice that, in principle, the forward–backward algorithm is not tailored to the DMP equations paradigm and can be used in the same context for a broader class of dynamical systems governed by nonlinear differential equations; however, implementing forward and backward steps through simulation of the dynamics may significantly increase the computational complexity of the overall algorithm. Another open problem is dealing with uncertainties within the presented framework. In realistic applications, the spreading parameters are never known with an absolute accuracy, but in a certain range, defined by the estimation error. Obviously, the optimization algorithm should be able to take these uncertainties into account. It would be useful to develop the robust version of our formulation, in the spirit of the setting known as robust influence maximization (80, 81).

Methods

DMP Equations. DMP belongs to the family of algorithms derived by using the cavity method of statistical physics and may be given an interpretation of passing messages along the graph edges. The obtained marginals are exact on tree graphs and asymptotically exact on sparse random networks. We provide an intuitive derivation of the DMP equations for the adopted modified SIR model, defined by Eqs. **1** and **2**. On a given instance of a network, these equations allow one to compute the marginal probability distributions $P^i_\sigma(t)$, where $\sigma \in \{S, I, R\}$ denotes the node state. The first key equation reads:

$$P^i_S(t) = P^i_S(0) \left(\prod_{t'=0}^{t-1} (1 - \nu_i(t'))(1 - \mu_i(t')) \right) \prod_{k \in \partial i} \theta^{k \to i}(t). \qquad [10]$$

It states the probability of node i to be susceptible at time t and is equal to the probability that i was in the S state at initial time $P^i_S(0)$ and remained so until time t. It neither changed states by following the ν and μ mechanisms (in brackets), nor by being infected by a neighbor (final term on right); the dynamic message $\theta^{k \to i}(t)$ has a meaning of the probability that node k did not pass an activation message to node i until time t. Strictly speaking, Eq. **10** is only valid on a tree graph; only in this case $\theta^{k \to i}(t)$ are independent for all $k \in \partial i$, so that the corresponding probability is factorized as in Eq. **10**. However, in practice, the decorrelation assumption holds to a good precision on general networks, even with small loops (see ref. 42 for in-depth discussions and supporting numerical experiments). The quantities $\theta^{k \to i}(t)$ are updated as follows:

$$\theta^{k \to i}(t) = \theta^{k \to i}(t-1) - \alpha_{ki} \phi^{k \to i}(t-1), \qquad [11]$$

which corresponds to the fact that $\theta^{k\to i}(t)$ can only decrease if an activation signal is passed along the directed link (ki); the corresponding probability equals the product of α_{ki} and the dynamic variable $\phi^{k\to i}(t-1)$, which has a meaning of the probability that node k is in the state I at time $t-1$, but has not infected node i until time $t-1$. To simplify further explanations, we introduce the dynamic messages $P_S^{k\to i}(t)$, $P_I^{k\to i}(t)$ and $P_R^{k\to i}(t)$, which denote the probabilities that node k is found at time t in the states S, I, or R, respectively, conditioned on node i remaining in state S. Alternatively, these variables can be thought of as the probabilities of k being susceptible, infected or recovered on a cavity graph, on which node i has been removed. Formally,

$$P_S^{k\to i}(t) = P_S^k(0)\left(\prod_{t'=0}^{t-1}(1-\nu_k(t'))(1-\mu_k(t'))\right)\prod_{l\in\partial k\setminus i}\theta^{l\to k}(t), \quad [12]$$

which coincides with the expression [**10**], except that $\theta^{i\to k}(t)$ is not included in the product on the right ($\partial k\setminus i$ denotes the set of neighbors of k without i). We also have

$$P_R^{k\to i}(t) = P_R^{k\to i}(t-1) + \mu_k(t-1)P_S^{k\to i}(t-1), \quad [13]$$

which expresses the monotonic increase of $P_R^{k\to i}(t)$ at each time step with the probability $\mu_k(t-1)P_S^{k\to i}(t-1)$, and

$$P_I^{k\to i}(t) = 1 - P_S^{k\to i}(t) - P_R^{k\to i}(t) \quad [14]$$

due to the normalization of probabilities. We are now ready to formulate the last relation which leads to the closure of the system of message-passing equations. The evolution of the message $\phi^{k\to i}(t)$ reads:

$$\phi^{k\to i}(t) = (1-\alpha_{ki})\phi^{k\to i}(t-1) + \Delta P_I^{k\to i}(t-1) \quad [15]$$

where $\Delta P_I^{k\to i}(t-1) \equiv P_I^{k\to i}(t) - P_I^{k\to i}(t-1)$. The physical meaning of Eq. **15** is as follows: $\phi^{k\to i}(t)$ decreases if the activation signal is actually transmitted (first term) and increases if node k transitions to the state I at the current time step. Eqs. **10**–**15** can be iterated in time starting from the given initial conditions $\{P_S^i(0), P_I^i(0), P_R^i(0)\}_{i\in V}$, with

$$\theta^{i\to j}(0) = 1, \quad \phi^{i\to j}(0) = \delta_{\sigma_i^0, I} = P_I^i(0). \quad [16]$$

The marginals $P_S^i(t)$ used throughout the text are obtained by using Eq. **10**, while $P_I^i(t)$ and $P_R^i(t)$ are computed via

$$P_R^i(t) = P_R^i(t-1) + \mu_i(t-1)P_S^i(t-1), \quad [17]$$

$$P_I^i(t) = 1 - P_S^i(t) - P_R^i(t). \quad [18]$$

The computational complexity of the DMP equations for solving the dynamics up to time T is given by $O(|E|T)$, where $|E|$ is the number of edges in the graph, which makes them scalable to sparse networks with millions of nodes. For spreading models other than SIR, DMP equations can be systematically derived from the initial dynamic transition rules, as shown in ref. 42.

Enforcing Dynamical Constraints and Backward Equations. The dynamics $\mathcal{D}$ and initial conditions $\mathcal{I}$ constraints are enforced in a similar way to that of $\mathcal{P}$ and the budget $\mathcal{B}$ constraints in Eqs. **7** and **8**. To each generic dynamic variable $\xi^i(t)$ and message $\chi^{k\to i}(t)$, we associate the corresponding Lagrange multipliers $\lambda_i^\xi(t)$ and $\lambda_{k\to i}^\chi(t)$, which enforce the relation between dynamic variables at subsequent times. For instance, the evolution of the quantities $\{P_R^i(t)\}_{i\in V}$ in the Lagrangian $\mathcal{L}$ is enforced via the term

$$\sum_{i\in V}\sum_{t=0}^{T-1}\lambda_i^R(t+1)\left[P_R^i(t+1) - P_R^i(t) - \mu_i(t)P_S^i(t)\right].$$

Variation with respect to the dual variables $\lambda_i^\xi(t)$ and $\lambda_{k\to i}^\chi(t)$ returns the forward DMP Eqs. **10**–**18**, while setting to zero the derivative of $\mathcal{L}$ with respect to the primal dynamic variables yields the relations between the Lagrange multipliers at subsequent times, which we interpret as the backward dynamic equations in our scheme. Similarly to Eqs. **10**–**15**, the backward equations have a distributed message-passing structure with linear computational complexity $O(|E|T)$ and are used to update the values of control parameters $\nu_i(t)$ and $\mu_i(t)$ at each iteration, taking into account the budget requirements [**6**]. Specifically, initializing the control parameters $\nu_i(t)$ and $\mu_i(t)$ to some arbitrary values (e.g., uniform over all nodes and times), we first propagate the DMP equations forward in time, up to the horizon T; then, using the existing primal parameter values, we fix end-point conditions for the dual parameters and propagate the equations for the dual parameters backward in time, updating the control parameters respecting the budget and variation constraints. These two steps are iterated for a predefined number of times or until global convergence of the process.

In the large-scale problems, where the algorithm explores the space of parameters by hopping from one solution to another, we choose a simple strategy: We run the forward–backward algorithm for several iterations for a range of values of the regularization parameter ϵ, which appears in the $\mathcal{P}$ block, and keep track of the best local optimum which provides the solution to the optimization problem after a maximum number of iterations (kept below the desired threshold which determines the computational complexity) is reached. The choice of ϵ impacts the type of solution obtained: Larger values of ϵ correspond to solutions where the budget is disseminated more uniformly across nodes, while smaller values lead to weight concentration on particular nodes. Depending on the application and the level of control over nodes, one type of solution can be preferred to another; this flexibility represents an attractive feature of the DMP algorithm. An explicit form of the Lagrangian for the problems considered in this work together with additional details is given in *SI Text*.

ACKNOWLEDGMENTS. We thank M. Chertkov, S. Misra, and M. Vuffray for fruitful discussions and valuable comments. A.Y.L. was supported by Laboratory Directed Research and Development Program at Los Alamos National Laboratory by the National Nuclear Security Administration of the US Department of Energy under Contract DE-AC52-06NA25396. D.S. was supported by Leverhulme Trust Grant RPG-2013-48.

1. Anderson RM, May RM, Anderson B (1992) *Infectious Diseases of Humans: Dynamics and Control* (Oxford Univ Press, Oxford), Vol 28.
2. Boccaletti S, Latora V, Moreno Y, Chavez M, Hwang DU (2006) Complex networks: Structure and dynamics. *Phys Rep* 424:175–308.
3. Rogers EM (2010) *Diffusion of Innovations* (Simon and Schuster, New York).
4. Pastor-Satorras R, Castellano C, Van Mieghem P, Vespignani A (2015) Epidemic processes in complex networks. *Rev Mod Phys* 87:925–979.
5. Federal Energy Regulatory Commission and North American Electric Reliability Corporation (2012) *Arizona - Southern California Outages on September 8, 2011: Causes and Recommendations* (Federal Energy Regulatory Commission and North American Electric Reliability Corporation, Washington, DC).
6. Dawood FS, et al. (2012) Estimated global mortality associated with the first 12 months of 2009 pandemic influenza a h1n1 virus circulation: A modelling study. *Lancet Infect Dis* 12:687–695.
7. US Government Accountability Office (2012) *Financial Regulatory Reform: Financial Crisis Losses and Potential Impacts of the Dodd-Frank Act* (Government Accountability Office, Washington, DC).
8. Lokhov AY, Lemons N, McAndrew TC, Hagberg A, Backhaus S (2016) Detection of cyber-physical faults and intrusions from physical correlations. *Proceedings of the 2016 IEEE 16th International Conference on Data Mining Workshops* (IEEE, New York), pp 303–310.
9. ALS Association (2016) ALS Ice Bucket Challenge. Available at www.alsa.org/fight-als/ice-bucket-challenge.html. Accessed August 31, 2016.
10. Rutledge P (2013) How Obama won the social media battle in the 2012 presidential campaign, The Media Psychology Blog. Available at mprcenter.org/blog/2013/01/how-obama-won-the-social-media-battle-in-the-2012-presidential-campaign/. Accessed August 31, 2016.
11. Epstein R, Robertson RE (2015) The search engine manipulation effect (seme) and its possible impact on the outcomes of elections. *Proc Natl Acad Sci USA* 112:E4512–E4521.
12. Margetts H, John P, Hale S, Yasseri T (2015) *Political Turbulence: How Social Media Shape Collective Action* (Princeton Univ Press, Princeton).
13. Domingos P, Richardson M (2001) Mining the network value of customers. *Proceedings of the Seventh ACM SIGKDD International Conference on Knowledge Discovery and Data Mining* (Association for Computing Machinery, New York), pp 57–66.
14. Martin KR, et al. (2013) Computational model for autophagic vesicle dynamics in single cells. *Autophagy* 9:74–92.
15. Csermely P, Korcsmáros T, Kiss HJ, London G, Nussinov R (2013) Structure and dynamics of molecular networks: A novel paradigm of drug discovery: A comprehensive review. *Pharmacol Therpeut* 138:333–408.
16. Jones S (2015) Army revives chindits as 'Facebook warriors' for smart battle. *Financ Times*. Available at https://www.ft.com/content/537c7436-a892-11e4-ad01-00144feab7de.
17. Pastor-Satorras R, Vespignani A (2002) Immunization of complex networks. *Phys Rev E* 65:036104.
18. Cohen R, Havlin S, Ben-Avraham D (2003) Efficient immunization strategies for computer networks and populations. *Phys Rev Lett* 91:247901.
19. Holme P, Kim BJ, Yoon CN, Han SK (2002) Attack vulnerability of complex networks. *Phys Rev E* 65:056109.
20. Holme P (2004) Efficient local strategies for vaccination and network attack. *Europhys Lett* 68:908–914.
21. Chen Y, Paul G, Havlin S, Liljeros F, Stanley HE (2008) Finding a better immunization strategy. *Phys Rev Lett* 101:058701.
22. Kitsak M, et al. (2010) Identification of influential spreaders in complex networks. *Nat Phys* 6:888–893.

23. Borge-Holthoefer J, Moreno Y (2012) Absence of influential spreaders in rumor dynamics. *Phys Rev E* 85:026116.
24. Hébert-Dufresne L, Allard A, Young JG, Dubé LJ (2013) Global efficiency of local immunization on complex networks. *Sci Rep* 3:2171.
25. Morone F, Makse HA (2015) Influence maximization in complex networks through optimal percolation. *Nature* 524:65–68.
26. Mugisha S, Zhou HJ (2016) Identifying optimal targets of network attack by belief propagation. *Phys Rev E* 94:012305.
27. Braunstein A, Dall'Asta L, Semerjian G, Zdeborová L (2016) Network dismantling. *Proc Natl Acad Sci USA* 113:12368–12373.
28. Altarelli F, Braunstein A, Dall'Asta L, Wakeling JR, Zecchina R (2014) Containing epidemic outbreaks by message-passing techniques. *Phys Rev X* 4:021024.
29. Altarelli F, Braunstein A, Dall'Asta L, Zecchina R (2013) Optimizing spread dynamics on graphs by message passing. *J Stat Mech Theor Exp* 2013:P09011.
30. Guggiola A, Semerjian G (2015) Minimal contagious sets in random regular graphs. *J Stat Phys* 158:300–358.
31. Kempe D, Kleinberg J, Tardos É (2003) Maximizing the spread of influence through a social network. *Proceedings of the Ninth ACM SIGKDD International Conference on Knowledge Discovery and Data Mining* (Association for Computing Machinery, New York), pp 137–146.
32. Chen W, Lakshmanan LV, Castillo C (2013) Information and Influence Propagation in Social Networks, *Synthesis Lectures on Data Management* (Morgan & Claypool, Williston, VT), Vol 5.
33. Du N, Song L, Gomez-Rodriguez M, Zha H (2013) Scalable influence estimation in continuous-time diffusion networks. *Adv Neural Inf Process Syst* 26:3147–3155.
34. Nowzari C, Preciado VM, Pappas GJ (2016) Analysis and control of epidemics: A survey of spreading processes on complex networks. *IEEE Control Syst* 36:26–46.
35. Borgs C, Chayes J, Ganesh A, Saberi A (2010) How to distribute antidote to control epidemics. *Random Struct Algorithm* 37(2):204–222.
36. Nian F, Wang X (2010) Efficient immunization strategies on complex networks. *J Theor Biol* 264(1):77–83.
37. Scaman K, Kalogeratos A, Vayatis N (2015) A Greedy Approach for Dynamic Control of Diffusion Processes in Networks. *Proceedings of the IEEE 27th International Conference on Tools with Artificial Intelligence (IEEE, New York),* pp 652–659.
38. Drakopoulos K, Ozdaglar A, Tsitsiklis JN (2014) An efficient curing policy for epidemics on graphs. *IEEE Trans Netw Sci Eng* 1:67–75.
39. Shapiro M, Delgado-Eckert E (2012) Finding the probability of infection in an SIR network is NP-hard. *Math biosciences* 240:77–84.
40. Karrer B, Newman MEJ (2010) Message passing approach for general epidemic models. *Phys Rev E* 82:016101.
41. Shrestha M, Moore C (2014) Message-passing approach for threshold models of behavior in networks. *Phys Rev E* 89:022805.
42. Lokhov AY, Mézard M, Zdeborová L (2015) Dynamic message-passing equations for models with unidirectional dynamics. *Phys Rev E* 91:012811.
43. le Cun Y, (1988) A theoretical framework for back-propagation. *Proceedings of the 1988 Connectionist Models Summer School*, eds Touresky D, Hinton G, Sejnowski T (Morgan Kaufman, San Mateo, CA), Vol 1, pp 21–28.
44. Saad D, Rattray M (1997) Globally optimal parameters for on-line learning in multilayer neural networks. *Phys Rev Lett* 79:2578.
45. Sebolt-Leopold JS, Herrera R (2004) Targeting the mitogen-activated protein kinase cascade to treat cancer. *Nat Rev Cancer* 4:937–947.
46. Roberts PJ, Der CJ (2007) Targeting the raf-mek-erk mitogen-activated protein kinase cascade for the treatment of cancer. *Oncogene* 26:3291–3310.
47. Gu S, et al. (2017) Optimal trajectories of brain state transitions. *NeuroImage* 148: 305–317.
48. Sahasrabudhe S, Motter AE (2011) Rescuing ecosystems from extinction cascades through compensatory perturbations. *Nat Commun* 2:170.
49. Suweis S, Simini F, Banavar JR, Maritan A (2013) Emergence of structural and dynamical properties of ecological mutualistic networks. *Nature* 500:449–452.
50. Allen F, Gale D (2000) Financial contagion. *J Polit Econ* 108:1–33.
51. Paga P, Kühn R (2015) Contagion in an interacting economy. *J Stat Mech Theor Exp* 2015:P03008.
52. Caccioli F, Shrestha M, Moore C, Farmer JD (2014) Stability analysis of financial contagion due to overlapping portfolios. *J Banking Finance* 46:233–245.
53. Lu W, Xu S, Yi X (2013) *Optimizing Active Cyber Defense in International Conference on Decision and Game Theory for Security* (Springer, New York), pp 206–225.
54. Kephart JO, White SR (1991) *Directed-graph epidemiological models of computer viruses. Proceedings of the IEEE Computer Society Symposium on in Research in Security and Privacy IEEE* (IEEE, New York), pp 343–359.
55. Maienhofer D, Finholt T (2002) Finding optimal targets for change agents: A computer simulation of innovation diffusion. *Comput Math Organ Theor* 8:259–280.
56. Pinto PC, Thiran P, Vetterli M (2012) Locating the source of diffusion in large-scale networks. *Phys Rev Lett* 109:068702.
57. Lokhov AY, Mézard M, Ohta H, Zdeborová L (2014) Inferring the origin of an epidemic with a dynamic message-passing algorithm. *Phys Rev E* 90:012801.
58. Altarelli F, Braunstein A, Dall'Asta L, Lage-Castellanos A, Zecchina R (2014) Bayesian inference of epidemics on networks via belief propagation. *Phys Rev Lett* 112: 118701.
59. Krebs VE (2002) Mapping networks of terrorist cells. *Connections* 24:43–52.
60. Choudhary P, Singh U (2015) A survey on social network analysis for counter-terrorism. *Int J Computer Appl* 112:14–29.
61. Knoke D (2015) *Emerging Trends in Social Network Analysis of Terrorism and Counterterrorism, Emerging Trends in the Social and Behavioral Sciences* (Wiley Online Library, New York).
62. Ushakov IA (2013) *Optimal Resource Allocation: With Practical Statistical Applications and Theory* (John Wiley & Sons, New York).
63. United Nations Office on Drugs and Crime (2012) *The Use of the Internet for Terrorist Purposes (United Nations, Vienna)*.
64. Klerks P (2001) The network paradigm applied to criminal organizations: Theoretical nitpicking or a relevant doctrine for investigators? Recent developments in The Netherlands. *Connections* 24:53–65.
65. De Domenico M, Porter MA, Arenas A (2015) Muxviz: A tool for multilayer analysis and visualization of networks. *J Complex Networks* 3:159–176.
66. Šubelj L, Bajec M (2011) Robust network community detection using balanced propagation. *The Eur Phys J B* 81:353–362.
67. Bu D, et al. (2003) Topological structure analysis of the protein–protein interaction network in budding yeast. *Nucleic Acids Res* 31:2443–2450.
68. Leskovec J, Kleinberg J, Faloutsos C (2007) Graph evolution: Densification and shrinking diameters. *ACM Trans Knowledge Discov Data* 1:2.
69. Boldi P, Codenotti B, Santini M, Vigna S (2004) UbiCrawler: A scalable fully distributed web crawler. *Software Pract Ex* 34:711–726.
70. Kribs-Zaleta CM, Velasco-Hernandez JX (2000) A simple vaccination model with multiple endemic states. *Math biosciences* 164:183–201.
71. Reluga TC, Medlock J (2007) Resistance mechanisms matter in SIR models. *Math Biosciences Eng* 4:553–563.
72. Hollingsworth TD, Ferguson NM, Anderson RM (2007) Frequent travelers and rate of spread of epidemics. *Emerging Infect Dis* 13:1288–1294.
73. Tatem AJ, Rogers DJ, Hay SI (2006) Global transport networks and infectious disease spread. *Adv Parasitol* 62:293–343.
74. Bureau of Transportation Statistics (2016) Bureau of Transportation Statistics. Available at https://www.transtats.bts.gov/DataIndex.asp. Accessed August 31, 2016.
75. Colizza V, Barrat A, Barthélemy M, Vespignani A (2006) The role of the airline transportation network in the prediction and predictability of global epidemics. *Proc Natl Acad Sci USA* 103:2015–2020.
76. Brockmann D, Helbing D (2013) The hidden geometry of complex, network-driven contagion phenomena. *Science* 342:1337–1342.
77. Epstein JM, et al. (2007) Controlling pandemic flu: The value of international air travel restrictions. *PLoS One* 2:e401.
78. Lokhov A (2016) Reconstructing parameters of spreading models from partial observations. *Adv Neural Inf Process Syst* 29:3467–3475.
79. Lokhov AY, Misiakiewicz T (2015) Efficient reconstruction of transmission probabilities in a spreading process from partial observations. arXiv:1509.06893.
80. He X, Kempe D (2016) Robust influence maximization. *Proceedings of the 22nd ACM SIGKDD International Conference on Knowledge Discovery and Data Mining* (Association for Computing Machinery, New York), pp 885–894.
81. Chen W, Lin T, Tan Z, Zhao M, Zhou X (2016) Robust influence maximization. *Proceedings of the 22nd ACM SIGKDD International Conference on Knowledge Discovery and Data Mining* (Association for Computing Machinery, New York), pp 795–804.
82. Doreian P, Mrvar A (1996) A partitioning approach to structural balance. *Social networks* 18:149–168.
83. Newman ME (2002) Spread of epidemic disease on networks. *Phys Rev E* 66:016128.
84. Granovetter M (1978) Threshold models of collective behavior. *Am J Sociol* 83: 1420–1443.
85. Morone F, Min B, Bo L, Mari R, Makse HA (2016) Collective influence algorithm to find influencers via optimal percolation in massively large social media. *Sci Rep* 6: 30062.
86. Hildebrand FB (1992) *Methods of Applied Mathematics* (Dover Publications, New York).